

## Novel Anatomic Mapping of Pelvic Plexus at Prostatic and Periprostatic Region on Fresh Frozen Cadaveric Setting

Emre Huri<sup>1</sup>, Mustafa F. Sargon<sup>2</sup>, Ilkan Tatar<sup>2</sup>, Makbule Cisel Aydın<sup>3</sup>, Mehmet Ezer<sup>1</sup>, Figen Söylemezoglu<sup>3</sup>

**Purpose:** We aimed to investigate the exact localization of neural pathway and the frequency of nerve fibers, which are located in the pelvic facial layers in the prostate and periprostatic regions.

**Materials and Methods:** We used four fresh frozen cadavers in this trial. Anatomical layers of anterior rectus fascia and abdominal rectus muscle were dissected to reach the retropubic area. Prostate, visceral and parietal pelvic fascia, levator ani muscle and puboprostatic ligaments were identified. Nine tissue samples, each 1x1 cm in size, were obtained from each cadaver and grouped separately. The locations of these samples are as follows. Group G I from 12 o'clock (apical region), G II from right prostatic apex, G III from 2 o'clock, G IV from right far pelvic lateral, G V from 5 o'clock, G VI from 7 o'clock, GVII from left far pelvic lateral, G VIII from 10 o'clock and G IX from left prostatic apex. Nerve distribution, frequency and diameters of these 9 groups were compared to each other.

**Results:** 36 specimens were obtained from 4 cadavers. Mean number of nerve fibers was 14.1. The number of nerve fibers in each location were not statistically different from each other ( $P = .9$ ). Mean nerve diameter was 89.1  $\mu$ m. Mean diameter of nerves was statistically different between groups II, III IV and VI and VIII ( $P = .001$ ). No difference was seen amongst others.

**Conclusion:** The distributions of nerve fibers at prostate and peri-prostatic region were homogeneous while the nerve diameters varied amongst the different regions.

**Keywords:** cadaver; cavernous nerve; neural mapping; pelvic plexus; prostate.

### INTRODUCTION

Pelvic Plexus or Inferior Hypogastric Plexus (IHP) is a diffuse neural network situated in periprostatic space covering the prostate. The nerve fibers and ganglia, that surround the prostate capsule, form this neural network. In these fields, nerve fibers course with the vascular structures as neuro-vascular bundle (NVB). NVB contains nerve fibers directly associated with prostate, seminal vesicle, all parts of urethra (prostatic, membranous and spongy), ejaculatory duct, cavernous and spongy bodies, bulbourethral gland and might be dissected anatomically from posterolateral surface of prostate.<sup>(1)</sup> These neural structures innervate the urogenital organs in the pelvic region. However, the main part of the IHP gives rise to the cavernous nerve (CN), which is responsible for erectile function. CN and IHP generally run in a caudal direction. The distribution of nerve fibers at the prostate level, adjacent tissues and far pelvic region is variable. Possessing knowledge of this distribution is important to achieve good functional outcomes following radical prostatectomy, which is a treatment modality for organ-confined prostate cancer. Nerve injuries can cause erectile dysfunction and incontinence after radical prostatectomy.<sup>(2)</sup> Nerve distribution of prostate gland and its' surrounding tissues is still a debated issue. In our study, after open pelvic cadaveric dissection, nerve distribution of

prostate gland and periprostatic tissue is analyzed based on their glandular location. We aimed to map the neural distribution of anterior, anterolateral, posterolateral sides of prostate, far lateral pelvic tissues and classify them according to their frequency and size parameters.

### MATERIALS AND METHODS

#### Preparation for Dissection

Four fresh frozen cadavers, having no previous dissection of the pelvic region, were included to the study. Cadavers were removed from the preservation tank one day prior to dissection, and then prepared accordingly. Open surgical set, sterile draping, retractors and optimal lighting systems were available. 2.5X surgical loop (HeineR) was used for fine dissection and surgical field control.

#### Dissection Technique

A urologist and an anatomist performed the dissections together. We performed retropubic radical prostatectomy as described by Walsh.<sup>(3)</sup> Subumbilical median incision was performed between pubic symphysis and umbilicus. After incision, each anatomic landmark was identified. They are as follows: skin, subcutaneous tissue, fascia of Camper, fascia of Scarpa, arcus tendineus of levator ani,, arcuate line of rectus sheath, semilunar line, fascia of rectus muscle, abdominal rectus muscle, transverse fascia, iliopsoas muscle, bladder,

<sup>1</sup>Department of Urology, Department of Urology, Hacettepe University School of Medicine, Ankara, Turkey.

<sup>2</sup>Department of Anatomy, Hacettepe University School of Medicine, Ankara, Turkey.

<sup>3</sup>Department of Pathology, Hacettepe University School of Medicine, Ankara, Turkey.

\*Correspondence: Hacettepe University, Faculty of Medicine, Department of Urology, 06100 Sıhhiye/Ankara/Turkey.

Phone: 0 312 305 19 69. E-mail: emrehuri@hacettepe.edu.tr.

Received October 2016 & Accepted August 2017

**Table 1.** Distribution of peripheric nerve fibers and their diameters according to the prostatic regions.

REGIONS (Group)	Number of Peripheric Nerves, n, *Mean ± SD (min-max)	Diameter of Peripheric Nerves, (µm), **Mean ± SD (min-max)
12 o'clock (G1)	13.2 ± 19.8 (0-42)	88.4 ± 45.1 (19-224)
Right apical (G2)	16.0 ± 20.8 (2-47)	79.5 ± 43.7 (16-189)
2 o'clock (G3)	18.7 ± 22.2 (4-51)	93.5 ± 111.6 (13-821)
Right lateral pelvic wall (G4)	12.0 ± 8.0 (3-21)	78.6 ± 51.3 (18-245)
5 o'clock (G5)	13.5 ± 11.1 (6-30)	100.5 ± 60 (35-344)
7 o'clock (G6)	19.2 ± 18.5 (5-46)	74.4 ± 42.5 (7-200)
Left lateral pelvic wall (G7)	9.5 ± 5.9 (2-16)	87.0 ± 56.0 (23-244)
10 o'clock (G8)	12.7 ± 13.2 (3-31)	121.5 ± 109.6 (39-608)
Left apical (G9)	12.0 ± 12.6 (0-28)	84.3 ± 64.7 (15-411)

\*p = 0.991 (SD = Standard Deviation)

prostate, perivesical space, superficial dorsal vein, deep dorsal vein, visceral pelvic fascia, parietal pelvic fascia, internal obturator muscle, levator ani muscle, prostatic fascia, prostatic capsul, Denonvillier's fascia, puboprostatic ligaments, pubovesical ligaments, arcus tendineus, seminal vesicles, vas deferens, cavernous penile nerve, external urethral sphincter and urethra.

**Tissue sampling and evaluation**

10x10 mm tissue samples were collected during the dissection from prostate and far prostate fields and put into 10% formaldehyde solution. Nine tissue samples were taken from each cadaver. Tissue samples classified to nine groups as GI to GIX. Tissue samples contain fascial tissues adjacent to prostate and further away from prostate. The location from which tissue samples were taken were planned so that all of the area between prostatic apex and vesicoprostatic junctions could be sampled. The fragments were made by considering clockwise anatomical neighborhoods, in this way tissue was removed from each area in equal proportions. Schematic illustration of clockwise sampling areas is shown in figure 1.

A total of nine tissue samples were taken. These samples were grouped clockwise. Samples were taken from 12 o'clock (group I), right apex (group II), 2 o'clock (group III), right lateral pelvic wall (group IV),

5 o'clock (group V), 7 o'clock (group VI), left lateral pelvic wall (group VII), 10 o'clock (group VIII) and left apex (group IX). The specimens were fixed in 10% formaldehyde solution and then, embedded into paraffin blocks. 5 µm thick sections from paraffin blocks were stained with H&E and visualized by one researcher with 100X magnification under the light microscope at department of pathology. In every section, diameter of the peripheral nerve fibers from pelvic plexus was measured and filed with oculometric method. The nerve fiber frequency according to different fields, its relation with dimensions of the fibers and diameter changes according to regions were evaluated statistically.

**Statistical analysis**

The post-hoc test reveals which specific groups cause the differences between groups. In this study, post-hoc test was performed to find the groups which make differences between the nerve diameters. Kruskal-Wallis test was used for comparing interregional nerve fiber numbers and one-way ANOVA was used for comparing nerve fibers diameters. P value was 0.05 and confidence bounds were 95%.

**RESULTS**

Thirty-six specimens were obtained from four cadavers. Mean nerve frequency in these groups were 13.2 (GI), 16 (GII), 18.7 (GIII), 12 (GIV), 13.5 (GV), 19.2 (GVI), 9.5 (GVII), 12.7 (GVIII) and 12 (GIX). Distribution of peripheral nerve fibers and their diameters of different prostatic regions are shown in Table 1. The frequency of nerve fibers in regions were not statistically different among groups (p = 0.991). The diameters of nerves were 88.4 (GI), 79.5 (GII), 93.5 (GIII), 78.6 (GIV), 100.5 (GV), 74.4 (GVI), 87 (GVII), 121.5 (GVIII), 84.3 (GIX) clockwise. Nerve diameters were significantly different between GVIII and GII (p = 0.04) and GVIII and GIII (p = 0.01), GVIII and GIV (p = 0.02), GVIII and GVI (p = 0.001) No significant difference was seen amongst the other groups. According to the microscopic analysis on the images, periprostatic nerve fiber diameters at 10 o'clock (GVIII) (Figure 2a) were higher than right prostatic apex (Figure 2b), 2 o'clock (GIII) (Figure 2c), right far lateral pelvic field (GIV) (Figure 2d), and 7 o'clock (Figure 2e) (GVI), respectively.

**DISCUSSION**

Our findings suggest that nerve fibers were distributed homogenously, which contradict with their results of the literature. However, we took samples from between ventrolateral and dorsolateral sides of the prostate. We didn't take samples from the ventral side. The reason

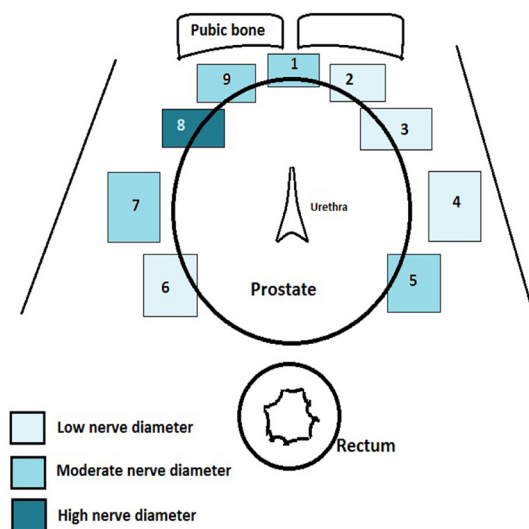


**Figure 1.** Schematic view of tissue sampling regions and difference between the regions for nerve fiber's diameters

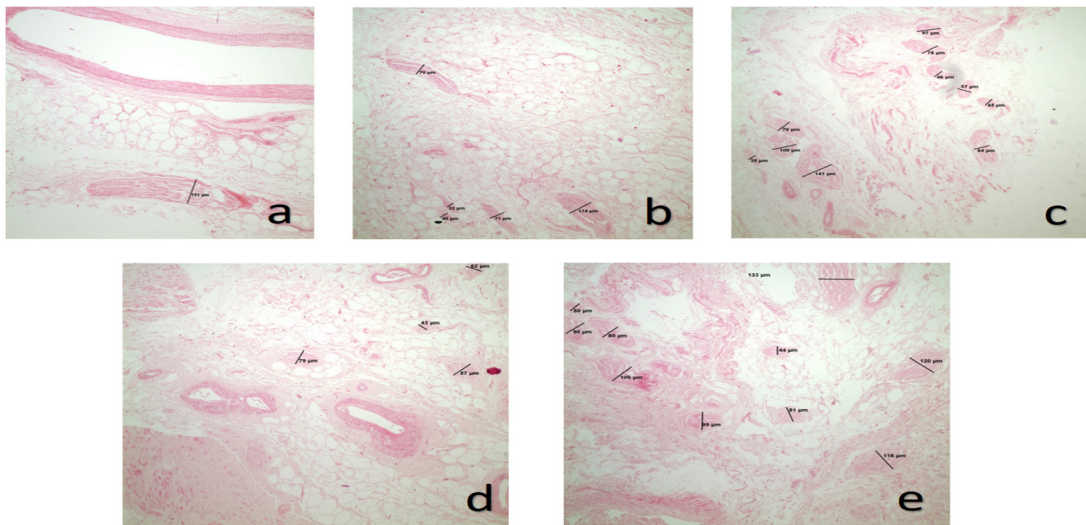


**Figure 2.**

- a. The light microscopic photograph of peripheral nerves at left 10 o'clock localization (G8-x10, H&E)
- b. The light microscopic photograph of peripheral nerves in the right prostatic apex (G2-x10, H&E)
- c. The light microscopic photograph of peripheral nerves at right 2 o'clock localization (G3-x10, H&E)
- d. The light microscopic photograph of peripheral nerves at right far lateral pelvic field (G6-x10, H&E)
- e. The light microscopic photograph of peripheral nerves at left 7 o'clock localization (G7-x10, H&E)

for that is the previous studies in literature clearly show that there is limited to no functional nerve fibers in the anterior region. We believe that the nerve distribution in our groups were similar due to our comparison of a different set of regions. Our findings also suggest that mean nerve diameter at 10 o'clock is higher than other regions. This is the first such finding in literature. Also, increased mean nerve diameter was higher in the left side, which shows that nerve distribution of the periprostatic area is not symmetric.

Since the first description radical prostatectomy by Walsh<sup>(4)</sup>, there has been important changes in nerve sparing radical prostatectomy technique.<sup>(3,5,6)</sup> These modifications increased functional and structural importance of anatomical landmarks. As of today, radical prostatectomy has satisfactory oncological outcomes. Although the long-term cancer-specific survival rate is high, it is clear that functional outcomes are still not satisfactory.<sup>(7)</sup> Different imaging techniques have been used to visualize the neurovascular bundle to improve the functional outcomes of radical prostatectomy.<sup>(8-10)</sup> Yadav et al. examined the prostate tissue of rats with a multiphotone microscope and showed that microscopic findings were similar to that of pathologic findings. They were able to visualize the neural fibers in the periprostatic region of the live tissue.<sup>(11)</sup> We have used light microscope for dissection and then sent the tissue for pathological analysis. However, our method is not proven to be a reliable method for visualization of nerve fibers.

Inferior hypogastric plexus is responsible for erection and urinary continence.<sup>(12)</sup> This plexus is made up of sympathetic and parasympathetic nerve fibers originating from T11-L2 and S3-4 segments of spinal cord. These nerve fibers make up cavernosal penile nerve at the distal end.<sup>(12,13)</sup> Clarebrough et al. reported that neu-

ral tissue is mainly posterolateral to prostate and nerve frequency decreased from the base of the prostate to the apex.<sup>(9)</sup> Ganzer et al. studied the topographic anatomy of prostate capsule and periprostatic nerve distribution. They have reported similar findings regarding the decreased nerve frequency at the prostatic apex. In addition, they reported that nerve frequency was higher at the ventrolateral and dorsal side of the prostate.<sup>(14)</sup> Other studies in literature have reported that nerve frequency decreased from the prostatic base to apex,<sup>(9,14-16)</sup> which contradicted with our results.

Kiyoshima et al. conducted a study in which they mapped the periprostatic nerve fibers. They used 79 prostatectomy specimens. In 52% of specimens, they have seen fat tissue between prostatic fascia and prostate capsule, and NVB was not identifiable. In 48% of specimens, prostatic fascia and prostate capsule were stuck to one another, and NVB could be identified. They also reported that periprostatic nerve anatomy varied between specimens.<sup>(17)</sup> Alsaied et al. used a computer enhanced anatomic dissection technique to visualize the neurovascular bundle. Their findings suggest that periprostatic nerve frequency of apex was higher in the anterior and anterolateral region.<sup>8</sup> Costello et al. performed a immunohistochemical investigation of periprostatic area. They have reported that the nerve frequency of anterior of prostate was minimal and consequently lateral dissection of prostate would be sufficient to spare the neurovascular bundle.<sup>18</sup> Similar to aforementioned studies, our results also show that the neural distribution of pelvic plexus varies from patient to patient. This anatomic variability of NVB could be used to explain why nerve-sparing is not successful in some patients.

The weakness of our study lies in the limited sample size. We didn't use a proven imaging method for vis-

ualization of NVB during dissection. In live surgery surgical instruments such as clips and thermal coagulation devices damage the neurovascular supply of the prostate and adjacent tissues. Since we used cold incisions for dissection, cadaveric setting enables us to do pathological analysis without the tissue damage. In our study, we didn't do an analysis of the nerve fibers of the prostatic capsule, however we believe that it should be the subject of a future study.

### CONCLUSIONS

The nerve fibers that originate from pelvic plexus are homogenously distributed in the periprostatic region. Mean nerve diameter is higher in the caudal region, towards the apex. Pelvic fascia is the key anatomic landmark for nerve-sparing during radical prostatectomy. A similarly conducted study with higher volume in a preferably live setting is needed to confirm these findings.

### CONFLICT OF INTERESTS

None of the contributing authors have any conflict of interest, including specific financial interest or relationship and affiliations relevant to the subject matter or materials discussed in the manuscript.

### REFERENCES

- Cumhur M, Y. N., Tuncel M: Temel Anatomi, 1 ed: ODTÜ Geliştirme Vakfı Yayıncılık ve İletişim A.Ş., p. 488, 2001
- Dauber, W., Feneis, H., Feneis, H. et al.: Pocket atlas of human anatomy founded by Heinz Feneis. In: Thieme ElectronicBook Library, 5th rev. ed. Stuttgart ; New York: Georg Thieme Verlag., p. 545 p., 2007
- Walsh, P. C.: Anatomic radical prostatectomy: evolution of the surgical technique. *J Urol*, 160: 2418, 1998
- Walsh, P. C.: Radical prostatectomy for the treatment of localized prostatic carcinoma. *Urol Clin North Am*, 7: 583, 1980
- Lepor, H.: A Review of Surgical Techniques for Radical Prostatectomy. *Reviews in Urology*, 7: S11, 2005
- Walsh, P. C., Marschke, P., Catalona, W. J. et al.: Efficacy of first-generation Cavermap to verify location and function of cavernous nerves during radical prostatectomy: a multi-institutional evaluation by experienced surgeons. *Urology*, 57: 491, 2001
- Haglund, E., Carlsson, S., Stranne, J. et al.: Urinary Incontinence and Erectile Dysfunction After Robotic Versus Open Radical Prostatectomy: A Prospective, Controlled, Nonrandomised Trial. *Eur Urol*, 68: 216, 2015
- Alsaid, B., Bessedé, T., Diallo, D. et al.: Division of autonomic nerves within the neurovascular bundles distally into corpora cavernosa and corpus spongiosum components: immunohistochemical confirmation with three-dimensional reconstruction. *Eur Urol*, 59: 902, 2011
- Clarebrough, E. E., Challacombe, B. J., Briggs, C. et al.: Cadaveric analysis of periprostatic nerve distribution: an anatomical basis for high anterior release during radical prostatectomy? *J Urol*, 185: 1519, 2011
- Walsh, P. C., Donker, P. J.: Impotence following radical prostatectomy: insight into etiology and prevention. *J Urol*, 128: 492, 1982
- Yadav, R., Mukherjee, S., Hermen, M. et al.: Multiphoton microscopy of prostate and periprostatic neural tissue: a promising imaging technique for improving nerve-sparing prostatectomy. *J Endourol*, 23: 861, 2009
- Mauroy, B., Demondion, X., Drizenko, A. et al.: The inferior hypogastric plexus (pelvic plexus): its importance in neural preservation techniques. *Surg Radiol Anat*, 25: 6, 2003
- Baader, B., Herrmann, M.: Topography of the pelvic autonomic nervous system and its potential impact on surgical intervention in the pelvis. *Clin Anat*, 16: 119, 2003
- Ganzer, R., Blana, A., Gaumann, A. et al.: Topographical anatomy of periprostatic and capsular nerves: quantification and computerised planimetry. *Eur Urol*, 54: 353, 2008
- Eichelberg, C., Erbersdobler, A., Michl, U. et al.: Nerve distribution along the prostatic capsule. *Eur Urol*, 51: 105, 2007
- Lee, S. B., Hong, S. K., Choe, G. et al.: Periprostatic distribution of nerves in specimens from non-nerve-sparing radical retropubic prostatectomy. *Urology*, 72: 878, 2008
- Kiyoshima, K., Yokomizo, A., Yoshida, T. et al.: Anatomical features of periprostatic tissue and its surroundings: a histological analysis of 79 radical retropubic prostatectomy specimens. *Jpn J Clin Oncol*, 34: 463, 2004
- Costello, A. J., Dowdle, B. W., Namdarian, B. et al.: Immunohistochemical study of the cavernous nerves in the periprostatic region. *BJU Int*, 107: 1210, 2011